A Reference Point-based Precise Relative Positioning Method Using a Single Frequency Receiver

Euiho Kim, Todd Walter, J. David Powell, *Stanford University*

BIOGRAPHY

Euiho Kim is a Ph.D. candidate in the Aeronautics and Astronautics Department at Stanford University. He received his B.S. in Aerospace Engineering in 2001 from Iowa State University and his M.S. from Stanford University in 2002. His research currently focuses on precise positioning using a single frequency receiver and flight inspection truth systems.

Dr. Todd Walter received his B. S. in physics from Rensselaer Polytechnic Institute and his Ph.D. in 1993 from Stanford University. He is currently a Senior Research Engineer at Stanford University. He is a co-chair of the WAAS Integrity Performance Panel (WIPP) focused on the implementation of WAAS and the development of its later stages. Key contributions include: early prototype development proving the feasibility of WAAS, significant contribution to MOPS design and validation, co-editing of the Institute of Navigation's book of papers about WAAS and its European and Japanese counterparts, and design of ionospheric algorithms for WAAS. He was the co-recipient of the 2001 ION early achievement award.

Prof. J. David Powell received his B.S. degree in Mechanical Engineering from MIT and his Ph.D in Aero/Astro from Stanford in 1970. He joined the Stanford Aero/Astro Department Faculty in 1971 and is currently an Emeritus Professor. Recent focus of research is centered around applications of GPS: applications of the FAA's WAAS for enhanced pilot displays, the use of WAAS and new displays to enable closer spacing on parallel runways, and the use of WAAS for flight inspection for conventional navigation aids. He has co-authored two text books in control systems design.

ABSTRACT

This paper investigates how to take advantage of the known position of a point at which a single frequency GPS receiver is located. Using this reference point and a single frequency receiver, a precise relative positioning method is developed. This method is particularly suited for the applications whose accuracy requirements are relaxed as time passes.

In some circumstances, one requires a far better accuracy than a single frequency receiver using standalone GPS or WAAS provides. Further, typical precise positioning methods such as differential GPS (DGPS), real time kinematic survey (RTK), and precise point positioning (PPP) cannot be used due to hardware or cost limitations. This difficult situation can be overcome with the new algorithm, precise relative positioning (PRP), described in this paper.

The PRP method requires raw measurements (e.g. pseudo ranges, carrier phase measurements, and ephemeris) from a single frequency receiver. It also requires a reference point. The reference point can be an initial position of a receiver (or any position during navigation for post-processing) that can be obtained by using various techniques, for example, the use of other sensors. The PRP has two modes. One is Iono-Free (I-F) PRP, the other one is Carrier-Based (C-B) PRP. The I-F PRP significantly mitigates the effect of multipath and ionosphere delays and cancels out user receiver clock errors by using combinations of pseudoranges and carrier phase measurements between satellites. On the other hand, C-B PRP uses only carrier phase measurement as ranging sources. Therefore, the I-F PRP can achieve better stability than standalone GPS or WAAS can provide, and the C-B PRP provides precise position solutions in a short-time application. The PRP is particularly well suited to the problems of accurate aircraft position determinations such as flight inspections. Preliminary results show a centimeter to decimeter level of stability in horizontal and vertical planes

1. INTRODUCTION

Precise positioning using GPS has been one of the most active research areas in the community of navigation because there have been many applications that require a high level of accuracy in position. The applications

include automatic aircraft landing, attitude determination, and autonomous control of land vehicles. Extensive studies on precise positioning driven by commercial and academic interests have resulted in successful methods and products.

One of the popular methods is Real-Time Kinematic (RTK) survey. RTK typically requires two or more receivers to cancel out the common errors between them. It also uses carrier phase measurements as ranging sources instead of code phase measurements. Therefore, a RTK system has a reference receiver, whose location is known, and one or more rover receivers. Also, a RTK system has a sophisticated integer ambiguity resolution algorithm in order to use carrier phase measurements as ranging sources. There are many implementations of ambiguity resolution. The robustness and effectiveness of the algorithms are important factors for the performance of a product [1]. With the help of error corrections from a reference receiver and the use of carrier phase measurements as ranging sources, current RTK systems usually achieve a centimeter level of accuracy. In addition to high accuracy, some RTK systems have the capability of an instant integer resolution [1] and of effectively handling cycle-slips [2], which provides robustness in various situation. Due to these advantages, RTK systems are widely used in many applications.

Another method is Precise Point Positioning (PPP) using a dual frequency receiver [3]. Unlike RTK, PPP depends on external sources like international GPS service (IGS) in order to mitigate the various errors in code or carrier phase measurements and orbital errors. Due to these error corrections from external sources, PPP does not require multiple receivers but needs a dual frequency receiver for accurate integer ambiguity resolutions. Using one receiver permits more flexible operations than RTK. However, latency or post processing is inevitable since the external sources are not available in real time. PPP provides a deci to centimeter level of accuracy in position domain.

Although these techniques can provide a high level of accuracy in position as well as a robust performance, it is not possible to use these methods in some applications such as a flight inspection truth system. The reason is that the FAA flight inspection truth system not only requires a high level of accuracy (up to 30cm 95%) but also near real time processing. In addition to that, flight inspection procedure can't afford the additional time in setting up local reference GPS receivers. Due to these requirements, RTK and PPP are not suited to this application. Therefore, in the current FAA flight truth inspection system, a navigation grade INS has been used as a main sensor with a radar altimeter and a vision sensor in order to achieve the requirements.

This paper presents a reference point-based precise relative positioning method using a single frequency receiver. It is motivated to enhance and reduce the cost of the current FAA flight inspection truth system by eliminating the expensive INS but achieves the same requirements with a single frequency receiver. In this method, it is assumed that a user is able to find the relative coordinates of a receiver to a reference point at one time during navigation by using other sensors. The absolute position of the reference point is also assumed to be surveyed. In a flight inspection procedure, a threshold on a runway serves as a reference point which is accurately surveyed. The onboard radar altimeter and vision sensors are used to find the relative position of an aircraft over the threshold. Figure 1 illustrates the procedure of the flight inspection and its position determination accuracy requirements. It should be also noted that the flight time is very short (less than 3 minutes) within the tight accuracy requirements. The new method is especially developed to take advantage of the known position of a receiver at one time and the short operation time.

The reference point-based precise relative positioning (PRP) method has two modes. One is Iono-Free PRP, and the other is Carrier-based PRP. The Iono-Free PRP provides stable position solutions with reduced multipath noise, which uses both code and carrier phase measurements and cancels out the ionospheric delays. On the other hand, the Carrier-based PRP provides very precise position solutions since it uses only carrier phase measurements. But, the carrier-based PRP has ionospheric delays and a large bias in the measurements. These different error characteristics of the two PRP modes can be utilized to satisfy the accuracy requirements of the flight inspection truth system, which will be discussed later.

This method can be implemented in real time or in post-processing. However, the relative position of a receiver to a reference point should be known at the initial time for a real time processing. For post-processing, the relative position to a reference point only needs to be provided at one time during navigation. The overall absolute position accuracy of this method is limited to the accuracy of the other sensors that is used to find the relative position to the reference point.

This paper is constructed as follows. The derivation of the I-F and C-B PRP will be shown in section 2. Also, the error characteristics of the two modes will be analyzed in that section. The results from the test of the two modes with static data will be shown in section 3. The conclusion will be followed in section 4.

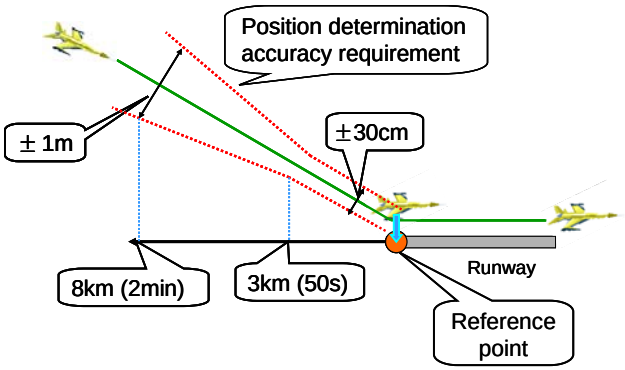

Figure 1: Illustration of FAA flight inspection truth system accuracy requirements and procedures in vertical plane

2. Derivation of Precise Relative Positioning Equations

There are two possible precise relative positioning solutions. One is Iono-Free (I-F) precise relative positioning (PRP), which is free of the ionospheric delays. The other one is carrier-based (C-B) precise relative positioning, which uses only carrier phase measurements as ranging sources.

2.1 Iono-Free (I-F) precise relative positioning

The GPS measurement for ranging sources are code phase measurements (ρ) and carrier phase measurements (Φ), which are

$$\rho^{(k)} = r^{(k)} + I^{(k)} + T^{(k)} + c(\delta t_u - \delta t_s^{(k)}) + \varepsilon_\rho^{(k)} \quad (2.1)$$

$$\Phi^{(k)} = r^{(k)} - I^{(k)} + T^{(k)} + c(\delta t_u - \delta t_s^{(k)}) + \lambda N^{(k)} + \varepsilon_\Phi^{(k)} \quad (2.2)$$

where the superscript *(k)* indicates the associated satellite. $r^{(k)}$ is the geometric range between a user and *k* th satellite. $I^{(k)}$ and $T^{(k)}$ are the ionospheric delays and the tropospheric delays respectively in the range measurements. δt_u is the receiver clock error, and $\delta t_s^{(k)}$ is the clock error of the satellite. $\varepsilon_\rho^{(k)}$ and $\varepsilon_\Phi^{(k)}$ denote the modeling error, multipath, and unmodeled effects in code and carrier phase measurements respectively. λ is the carrier wavelength on L1, and $N^{(k)}$ is the integer ambiguity on L1 of the satellite.

The ionospheric delays are cancelled out by summing the halves of the code phase measurements and the carrier phase measurements as follows.

$$\begin{aligned} y^{(k)} &= \tfrac{1}{2}\rho^{(k)} + \tfrac{1}{2}\Phi^{(k)} \\ &= r^{(k)} + T^{(k)} + c(\delta t_u - \delta t_s^{(k)}) + \tfrac{1}{2}\lambda N^{(k)} \\ &\quad + \tfrac{1}{2}\varepsilon_\rho^{(k)} + \tfrac{1}{2}\varepsilon_\Phi^{(k)} \end{aligned} \quad (2.3)$$

The tropospheric delays can be compensated from the current high fidelity troposphere models [4]. Satellite clock error corrections can be computed by using GPS ephemeris data or with WAAS data. With these error corrections, equation (2.3) becomes

$$\begin{aligned} y^{(k)} - \hat{T}^{(k)} + c\delta\hat{t}_s^{(k)} &= r^{(k)} + c\delta t_u + \tfrac{1}{2}\lambda N^{(k)} \\ &\quad + \tfrac{1}{2}\varepsilon_\rho^{(k)} + \tfrac{1}{2}\varepsilon_\Phi^{(k)} + \varepsilon_T^{(k)} + \varepsilon_{t_s}^{(k)} \end{aligned} \quad (2.4)$$

where $\varepsilon_T^{(k)}$ and $\varepsilon_{t_s}^{(k)}$ stand for the residual errors of the tropospheric delays and the satellite clock error corrections. $\hat{T}$ is the estimated tropospheric delays, and $\delta\hat{t}_s$ is the estimated satellite clock error.

At this point, let us designate a reference point, p_{ref} whose absolute position is assumed to be surveyed. The position of a user at any time can be described as the sum of the position of the reference point and the relative position to the reference point, δp, as follows.

$$p_{user} = p_{ref} + \delta p \quad (2.5)$$

where p_{user} is the position of a user.

The geometric range between the reference point and a satellite, r_R, can be easily computed since the absolute position of the reference point is known. It is well known that when the baseline of the reference point and the receiver is short (~10km) compared to the distance to the *k* th satellite, the difference between the geometric ranges to the satellite from the user, $r^{(k)}$,and the reference point, $r_R^{(k)}$, can be described as [5]

$$r^{(k)} - r_R^{(k)} = -1^{(k)} \bullet \delta p \quad (2.6)$$

$1^{(k)}$ is the line of sight vector to k th satellite from the reference point. This situation is illustrated in Figure 2.

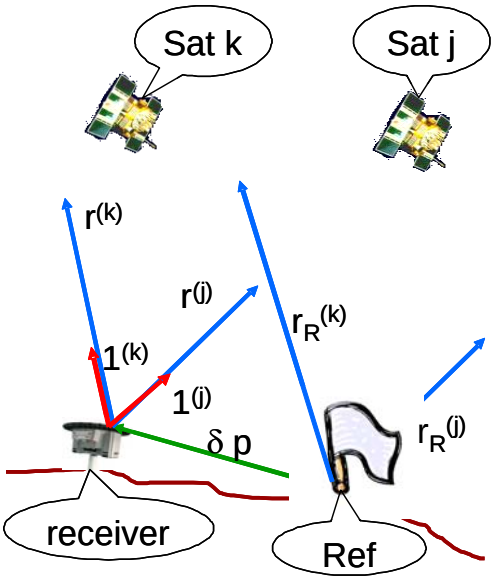

Figure 2: Geometry of a receiver and a reference point

Therefore, if $r_R^{(k)}$ is subtracted from equation (2.4), then

$$\begin{aligned}\tilde{y}^{(k)} &= y^{(k)} - r_R^{(k)} - \hat{T}^{(k)} + c\delta\hat{t}_s^{(k)} \\ &= -1^{(k)}\bullet\delta p + c\delta t_u + \tfrac{1}{2}\lambda N^{(k)} \\ &\quad + \tfrac{1}{2}\varepsilon_\rho^{(k)} + \tfrac{1}{2}\varepsilon_\Phi^{(k)} + \varepsilon_T^{(k)} + \varepsilon_{t_s}^{(k)}\end{aligned} \tag{2.7}$$

Let us subtract $\tilde{y}^{(j)}$ from $\tilde{y}^{(k)}$ in order to cancel out the receiver clock error, then

$$\begin{aligned}\tilde{y}^{(k,j)} &= \tilde{y}^{(k)} - \tilde{y}^{(j)} \\ &= (-1^{(k)} + 1^{(j)})\bullet\delta p + \tfrac{1}{2}\lambda N^{(k,j)} \\ &\quad + \tfrac{1}{2}\varepsilon_\rho^{(k,j)} + \tfrac{1}{2}\varepsilon_\Phi^{(k,j)} + \varepsilon_T^{(k,j)} + \varepsilon_{t_s}^{(k,j)}\end{aligned} \tag{2.8}$$

where $(\bullet)^{(k,j)}$ denotes $(\bullet)^{(k)} - (\bullet)^{(j)}$.

There are two unknowns, δp and $N^{(k,j)}$, in equation (2.8) except the noise terms. Since it is assumed that δp is known at one time during navigation, it is possible to approximately evaluate $N^{(k,j)}$ at that particular time. Let us denote the estimated relative position to the reference point from other sensors as $\delta\hat{p}_s$. Then, the integer ambiguity terms can be approximated as

$$\begin{aligned}\tfrac{1}{2}\lambda\hat{N}^{(k,j)} &= \tilde{y}^{(k,j)} - (-1^{(k)} + 1^{(j)})\bullet\delta\hat{p}_s \\ &= -(-1^{(k)} + 1^{(j)})\bullet b_p + \tfrac{1}{2}\lambda N^{(k,j)} \\ &\quad + \tfrac{1}{2}\varepsilon_\rho^{(k,j)} + \tfrac{1}{2}\varepsilon_\Phi^{(k,j)} + \varepsilon_T^{(k,j)} + \varepsilon_{t_s}^{(k,j)}\end{aligned} \tag{2.9}$$

where $b_p = \delta\hat{p}_s - \delta p$. b_p is the error in $\delta\hat{p}_s$ caused by the other sensors which is used to find the relative position to the reference point. Therefore, the value of b_p depends on the accuracy of the other sensors. $\hat{N}^{(k,j)}$ is the estimated integer ambiguity terms. $\hat{N}^{(k,j)}$ has offsets because of b_p and the noise terms. Therefore, $\frac{1}{2}\lambda\hat{N}^{(k,j)}$ can be described as

$$\tfrac{1}{2}\lambda\hat{N}^{(k,j)} = \tfrac{1}{2}\lambda N^{(k,j)} + b_{N^{(k,j)}} \tag{2.10}$$

where $b_{N^{(k,j)}}$ is

$$\begin{aligned}b_{N^{(k,j)}} &= -(-1^{(k)} + 1^{(j)})\bullet b_p + \tfrac{1}{2}\varepsilon_\rho^{(k,j)} + \tfrac{1}{2}\varepsilon_\Phi^{(k,j)} \\ &\quad + \varepsilon_T^{(k,j)} + \varepsilon_{t_s}^{(k,j)}\end{aligned} \tag{2.11}$$

$b_{N^{(k,j)}}$ is the bias in the estimated integer terms, and it is closely related to the position error characteristics. This issue will be discussed in the analysis of the error characteristics of the I-F and C-B precise relative positioning solutions.

Now, it is possible to solve for δp by subtracting $\frac{1}{2}\lambda\hat{N}^{(k,j)}$ from equation (2.8) as follows.

$$\tilde{y}^{(k,j)} - \tfrac{1}{2}\lambda\hat{N}^{(k,j)} = (-1^{(k)} + 1^{(j)})\bullet\delta p + \varepsilon_{total}^{(k,j)} \tag{2.12}$$

where

$$\varepsilon_{total}^{(k,j)} = \tfrac{1}{2}\varepsilon_\rho^{(k,j)} + \tfrac{1}{2}\varepsilon_\Phi^{(k,j)} + \varepsilon_T^{(k,j)} + \varepsilon_{t_s}^{(k,j)} - b_{N^{(k,j)}} \tag{2.13}$$

It is easy to construct a system of linear equation by implementing the same procedures for the other satellites in order to solve for δp in the least square sense. But, rather than solving the system of equations similar to equation (2.12), it may be better to further reduce the multipath noise by using a Hatch filter. In this case, the carrier smoothed pseudo range, $\rho_s^{(k)}(t_i)$, can be used in stead of $\rho^{(k)}(t_i)$, which is

$$\begin{aligned}\rho_s^{(k)}(t_i) &= \tfrac{1}{M}\rho^{(k)}(t_i) + \tfrac{M-1}{M}[\rho_s^{(k)}(t_{i-1}) + \\ &\quad \left(\Phi^{(k)}(t_i) - \Phi^{(k)}(t_{i-1})\right)]\end{aligned} \tag{2.14}$$

where M is the number of epochs of the measurements that are used for smoothing. The use of $\rho_s^{(k)}(t_i)$ makes equation (2.3) invalid because the ionospheric delays are not exactly cancelled out. Therefore, a small number for M is desirable in order for the derived equations to be

reasonable. The value of M may vary with respect to the activity of the ionosphere and multipath.

With the determined integer ambiguity terms and the smoothed pseudo ranges, the I-F precise relative positioning equation for k number of satellites can be described in as

$$\underbrace{\begin{bmatrix} \tilde{y}_s^{(1,j)} - \frac{1}{2}\lambda\hat{N}^{(1,j)} \\ \tilde{y}_s^{(2,j)} - \frac{1}{2}\lambda\hat{N}^{(2,j)} \\ \vdots \\ \tilde{y}_s^{(k,j)} - \frac{1}{2}\lambda\hat{N}^{(k,j)} \end{bmatrix}_t}_{Y(t)} = \underbrace{\begin{bmatrix} -1^{(1)} + 1^{(j)} \\ -1^{(2)} + 1^{(j)} \\ \vdots \\ -1^{(k)} + 1^{(j)} \end{bmatrix}_t}_{H(t)} \delta p(t) + \begin{bmatrix} \varepsilon_{total,s}^{(1,j)} \\ \varepsilon_{total,s}^{(2,j)} \\ \vdots \\ \varepsilon_{total,s}^{(k,j)} \end{bmatrix}_t \quad (2.15)$$

where the subscript s denotes the carrier-smoothed measurements. There is no combination of the same satellite, such as $(\bullet)^{(j,j)}$.

Various weighting matrix can also be constructed for the equation (2.15). Then, the relative position with respect to the reference point can be estimated with weighted least squares as follows.

$$\delta\hat{p}_{IF}(t) = \left(H^T(t)W(t)H(t)\right)^{-1} H^T(t)W(t)Y(t) \quad (2.16)$$

The error characteristics of $\delta\hat{p}_{IF}$ will be discussed in the later section.

2.2 Carrier-based (C-B) precise relative positioning

Since the integer ambiguities, $N^{(k,j)}$, are solved in the process of I-F precise relative positioning, it is possible to use only the carrier phase measurements as ranging sources. The similar procedures to the I-F precise relative positioning algorithm can be applied for the C-B precise relative positioning as follows.

At first, let us apply the troposphere and the satellite clock error corrections to the carrier phase measurements. Also, Subtracting $r_R^{(k)}$ from the carrier phase measurements results in

$$\begin{aligned} \tilde{z}^{(k)} &= \Phi^{(k)} - r_R^{(k)} - \hat{T}^{(k)} + c\delta\hat{t}_s^{(k)} \\ &= -1^{(k)} \bullet \delta p - I^{(k)} + c\delta t_u + \lambda N^{(k)} \\ &\quad + \varepsilon_\Phi^{(k)} + \varepsilon_T^{(k)} + \varepsilon_{t_s}^{(k)} \end{aligned} \quad (2.17)$$

Then, the difference between $\tilde{z}^{(k)}$ and $\tilde{z}^{(j)}$ is

$$\begin{aligned} \tilde{z}^{(k,j)} &= \tilde{z}^{(k)} - \tilde{z}^{(j)} \\ &= \left(-1^{(k)} + 1^{(j)}\right) \bullet \delta p - I^{(k,j)} + \lambda N^{(k,j)} \\ &\quad + \varepsilon_\Phi^{(k,j)} + \varepsilon_T^{(k,j)} + \varepsilon_{t_s}^{(k,j)} \end{aligned} \quad (2.18)$$

Now, let us apply the estimated integer terms to the above equation. Then,

$$\begin{aligned} \tilde{z}^{(k,j)} - \lambda\hat{N}^{(k,j)} &= \left(-1^{(k)} + 1^{(j)}\right) \bullet \delta p - I^{(k,j)} \\ &\quad - 2b_{N^{(k,j)}} + \varepsilon_\Phi^{(k,j)} + \varepsilon_T^{(k,j)} + \varepsilon_{t_s}^{(k,j)} \end{aligned} \quad (2.19)$$

A system of linear equations similar to the equation (2.19) for the other satellites can be described as

$$\underbrace{\begin{bmatrix} \tilde{z}^{(1,j)} - \lambda\hat{N}^{(1,j)} \\ \tilde{z}^{(2,j)} - \lambda\hat{N}^{(2,j)} \\ \vdots \\ \tilde{z}^{(k,j)} - \lambda\hat{N}^{(k,j)} \end{bmatrix}_t}_{Z(t)} = \underbrace{\begin{bmatrix} -1^{(1)} + 1^{(j)} \\ -1^{(2)} + 1^{(j)} \\ \vdots \\ -1^{(k)} + 1^{(j)} \end{bmatrix}_t}_{H(t)} \delta p(t) + \begin{bmatrix} \varepsilon_{total,\Phi}^{(1,j)} \\ \varepsilon_{total,\Phi}^{(2,j)} \\ \vdots \\ \varepsilon_{total,\Phi}^{(k,j)} \end{bmatrix}_t \quad (2.20)$$

where

$$\varepsilon_{total,\Phi}^{(k,j)} = -I^{(k,j)} - 2b_{N^{(k,j)}} + \varepsilon_\Phi^{(k,j)} + \varepsilon_T^{(k,j)} + \varepsilon_{t_s}^{(k,j)} \quad (2.21)$$

Of course, there in no combination of the same satellite.

The relative position with respect to the reference point can be solved from

$$\delta\hat{p}_{CB}(t) = \left(H^T(t)W(t)H(t)\right)^{-1} H^T(t)W(t)Z(t) \quad (2.22)$$

The error characteristics of $\delta\hat{p}_{CB}$ will be discussed in the next section.

2.3 The error characteristics of I-F and C-B precise relative positioning solutions

I-F and C-B precise relative positioning (PRP) solutions have different error characteristics. These different error characteristics imply when to use either I-F or C-B position solutions.

Equation (2.13) shows the various error terms in the measurements for the I-F PRP. Let us restate equation (2.13) as a function of time as follows.

$$\begin{aligned} \varepsilon_{total}^{(k,j)}(t) &= \tfrac{1}{2}\varepsilon_\rho^{(k,j)}(t) + \tfrac{1}{2}\varepsilon_\Phi^{(k,j)}(t) + \varepsilon_T^{(k,j)}(t) \\ &\quad + \varepsilon_{t_s}^{(k,j)}(t) - b_{N^{(k,j)}}(0) \end{aligned} \quad (2.23)$$

where

$$b_{N^{(k,j)}}(0) = -(-1^{(k)} + 1^{(j)})\bullet b_p(0) + \tfrac{1}{2}\varepsilon_\rho^{(k,j)}(0) + \tfrac{1}{2}\varepsilon_\Phi^{(k,j)}(0) + \varepsilon_T^{(k,j)}(0) + \varepsilon_{t_s}^{(k,j)}(0) \quad (2.24)$$

The time, t, indicates the elapsed time from the time, 0, when the differenced integer terms are resolved. In equation (2.23), $\varepsilon_T^{(k,j)}(t)$ and $\varepsilon_{t_s}^{(k,j)}(t)$ do not significantly change over time [5]. Therefore, $\varepsilon_T^{(k,j)}(0)$ and $\varepsilon_{t_s}^{(k,j)}(0)$ in $b_{N^{(k,j)}}(0)$ actually mitigate the residual tropospheric delays and the satellite clock errors over short time (~tens of minutes). $\frac{1}{2}\varepsilon_\Phi^{(k,j)}(\bullet)$ can be ignored since it is very small compared to the other terms. Therefore, equation (2.23) can be approximated over short time as follows.

$$\varepsilon_{total}^{(k,j)}(t) \approx \tfrac{1}{2}\varepsilon_\rho^{(k,j)}(t) + (-1^{(k)} + 1^{(j)})\bullet b_p(0) - \tfrac{1}{2}\varepsilon_\rho^{(k,j)}(0) = \tfrac{1}{2}\varepsilon_\rho^{(k,j)}(t) + b_{IF} \quad (2.25)$$

where b_{IF} is the bias due to inaccurate determination of the relative position to the reference point and multipath when the integer terms are resolved. Of course, $\varepsilon_{total}^{(k,j)}(t)$ will have a larger but fixed bias when time increases such that $\varepsilon_T^{(k,j)}(0)$ and $\varepsilon_{t_s}^{(k,j)}(0)$ do not effectively mitigate $\varepsilon_T^{(k,j)}(t)$ and $\varepsilon_{t_s}^{(k,j)}(t)$. The magnitude of b_{IF} depends on the multipath and the accuracy of other sensors which are used to find the relative position to the reference point. $\sigma_{b_{IF}}$ can be approximated as follows.

$$\sigma_{b_{IF}} \approx \sqrt{2\sigma_{b_p}^2 + \tfrac{1}{2}\sigma_\rho^2} \quad (2.26)$$

where σ_{b_p} is the rms of other sensors, and σ_ρ the rms range error due to multipath. Therefore, the preciseness of the I-F PRP depends on the accuracy of the other sensors and multipath. The rms of $\varepsilon_{total}^{(k,j)}(t)$ is quite small compared to the rms of the errors the code phase measurement. This is mainly due to the eliminated (or nearly eliminated if carrier-smoothing is used) ionospheric delays and the reduced multipath effect.

On the other hand, the equation (2.21) shows the error terms in the measurements for the C-B PRP. Let us restate the equation (2.21) as a function of time as follows.

$$\varepsilon_{total,\Phi}^{(k,j)}(t) = -I^{(k,j)}(t) - 2b_{N^{(k,j)}}(0) + \varepsilon_\Phi^{(k,j)}(t) + \varepsilon_T^{(k,j)}(t) + \varepsilon_{t_s}^{(k,j)}(t) \quad (2.27)$$

Equation (2.27) can be approximated over short time (~tens of minutes) as follows.

$$\varepsilon_{total,\Phi}^{(k,j)}(t) \approx -I^{(k,j)}(t) + 2(-1^{(k)} + 1^{(j)})\bullet b_p(0) - \varepsilon_\rho^{(k,j)}(0) - \varepsilon_T^{(k,j)}(0) - \varepsilon_{t_s}^{(k,j)}(0) = -I^{(k,j)}(t) - b_{CB} \quad (2.28)$$

where b_{CB} is the bias caused by inaccurate determination of the integer ambiguities. $\varepsilon_{total,\Phi}^{(k,j)}(t)$ will be larger but fixed as time increases like $\varepsilon_{total}^{(k,j)}(t)$. $\sigma_{b_{IF}}$ can be approximated as follows.

$$\sigma_{b_{CB}} \approx \sqrt{8\sigma_{b_p}^2 + 2\sigma_\rho^2 + 2\sigma_T^2 + 2\sigma_{t_s}^2} \quad (2.29)$$

Apparently, $\varepsilon_{total,\Phi}^{(k,j)}(t)$ is much lager than $\varepsilon_{total}^{(k,j)}(t)$. Therefore, it is highly likely that the measurements for the C-B PRP may have a lager bias than I-F PRP. It is proved in the analysis that the quality of other sensors used to find the relative position to the reference point effects the performance of I-F PRP and C-B PRP since any offsets caused by the other sensor will remain as a bias in the range measurement.

It is clearly shown that I-F PRP provides better performance the C-B PRP. The main drawback of the C-B PRP is that the uncompensated ionospheric delays and the large bias in the measurements, b_{CB}, may introduce drift-like errors in position domain in a few tens of minutes. However, the C-B PRP results in smooth solutions since there is little multipath in the measurements. Furthermore, the C-B position solution is more precise closer to the beginning. This is mostly due to that the differential delay of the ionosphere does not rapidly change over time. Therefore, it could be desirable to use the C-B PRP solution near the beginning of the operation time and use I-F PRP later. The transition time to C-B PRP to I-F PRP can be determined from the field test, but it won't be discussed in this paper.

It should be noted that the C-B relative position solutions do not match to the surveyed relative position to the reference point when the operation time is 0. This is caused by the remaining error terms in the equation (2.28) when the time is 0. The offset can be computed from the C-B relative position solution and the surveyed relative position at time 0. This offset will be calibrated for the entire C-B relative position solution.

2.4 Satellite constellation change and cycle-slips

It is likely that a new satellite comes after the resolution of the difference integer terms, $N^{(k,j)}$, at the initial time. At this time, the accurate relative position from a receiver to the reference point may not be available. One possible

option to deal with a new satellite is to use $\delta\hat{p}$ instead of $\delta\hat{p}_s$ in order to obtain a new $N^{(k,j)}$. The effect of using $\delta\hat{p}$ is that the new $N^{(k,j)}$ is more likely to have a larger bias than other differenced integer terms. It also may cause a sudden jump in the position domain, which is not desirable for the purpose of precise positioning. One trick to avoid the sudden jump is to compute positions with and without a new satellite at this particular epoch. The difference between the two position solutions is defined to be a calibration factor. The position solution with the new satellite in the future will be calibrated to the calibration factor. It is also possible that a satellite disappears during the navigation period. Usually, a sudden jump in position domain is also observed when a satellite disappears. What needs to be done in this case is to re-compute the position at the previous epoch with and without the lost satellites and compute the calibration factor. Then, the calibration factor will be applied to the future position solutions. Another possible situation is a cycle-slip. A cycle-slipped satellite can be treated like a satellite that disappears and comes back immediately. It should be noted that this simple calibration technique is particularly useful for a short time operation because the jump acts like a bias in short time. The overuse of this calibration technique for a long time may degrade the performance of the I-F PRP and C-B PRP.

3. RESULTS

The proposed algorithms are processed with static receiver data. The data were taken with a Novatel antenna at Stanford University in March, 2005. The reference point is set to be the position of the antenna whose position is accurately (better than a few centimeters) surveyed. The sampling rate of the data was 1 second, and 20 seconds of carrier-smoothing is used for the I-F PRP. The I-F PRP and the C-B PRP performances for the 10 minutes of operation time are compared. Then, I-F PRP is processed for 1 hour operation time, and it is compared with the standalone GPS.

3.1 Comparison of the performance of I-F PRP and C-B PRP for 10 minutes operation time

The I-F PRP and the C-B PRP algorithms are processed with 40 data sets of 10 minutes operation. Also, standalone GPS position solutions are processed for these tests. Figure 3 and 4 shows the horizontal and vertical position errors.

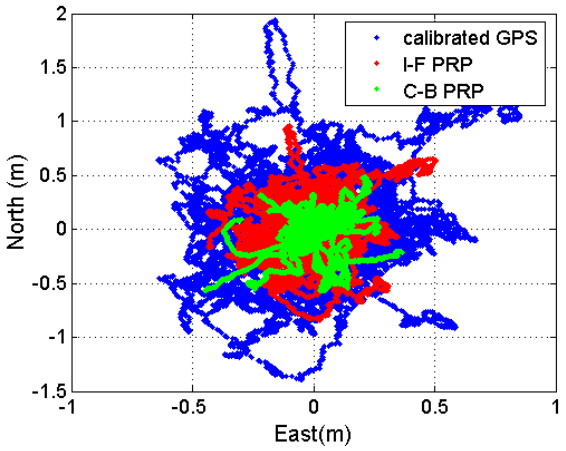

Figure 3: Horizontal position errors in East and North of I-F PRP and C-B PRP

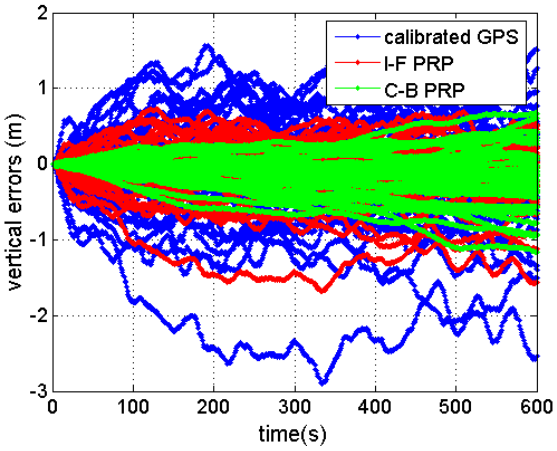

Figure 4: Vertical position errors of I-F PRP and C-B PRP

The position solutions from standalone GPS are calibrated to the position of the reference point at the initial time in order to compare the stabilities of standalone GPS and PRP algorithms. The I-F PRP provides noisier position solutions than C-B PRP but it is more stable than C-B PRP over time. I-F PRP solutions are less noisy than the calibrated GPS position. The distinct error characteristics of C-B PRP is that the position error is quite small near to the beginning and becomes larger as time passes, which is expected from the section **2.3.** Overall, C-B PRP provides the best performance among the three position solutions over 10 minutes of operation time. The number of satellites remains the same, and no cycle-slips are observed for each operation.

3.2 The performance of I-F precise relative positioning for 1 hour operation time

The results in horizontal and vertical of the I-F PRP and standalone GPS with 11 data sets of 1hour operation time are shown in Figure (5) and (6). The number of satellites is shown in Figure (7), and no cycle-slip is observed.

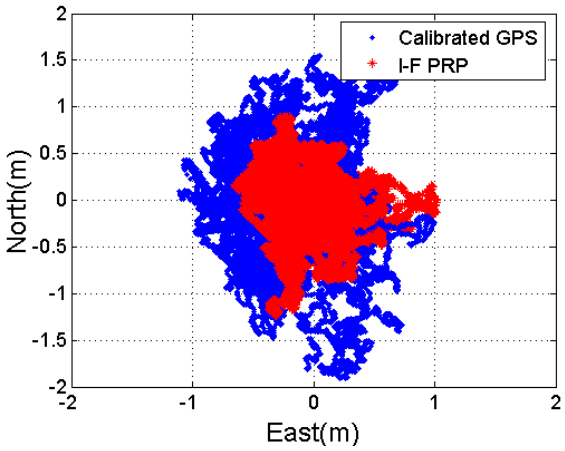

Figure 5: Horizontal Error in 11 data sets for 1 hour operation

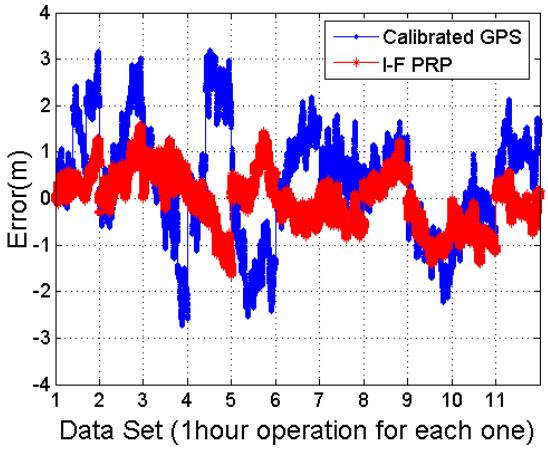

Figure 6: Vertical Error in 11 data sets for 1 hour operation

It is clearly shown in figure (5) and (6) that the I-F PRP provides significantly better stability than standalone GPS over 1 hour operation time. The position errors most of time are less than 1m both in horizontal and vertical. The mean, variance, and root-mean-square (RMS) values for the positioning errors of standalone GPS and I-F PRP in figures (5) and (6) are shown in figures (8), (9), (10), (11), (12) and (13).

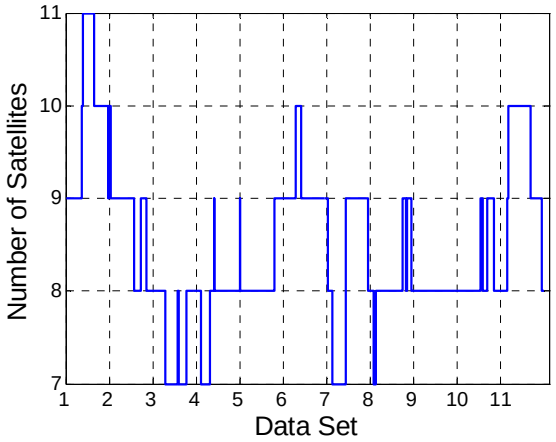

Figure 7: The number of satellites in 11 data sets for 1 hour operation

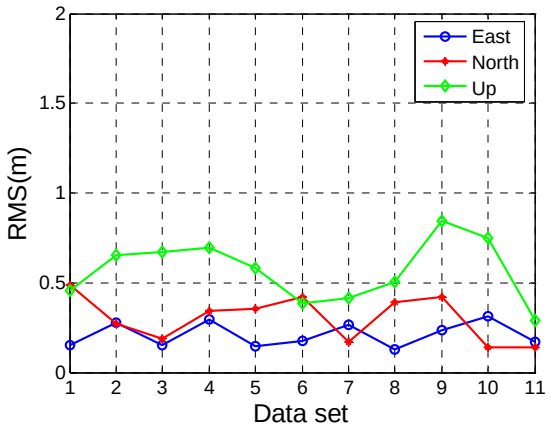

Figure 8: RMS of I-F PRP in 11 data sets for 1 hour operation

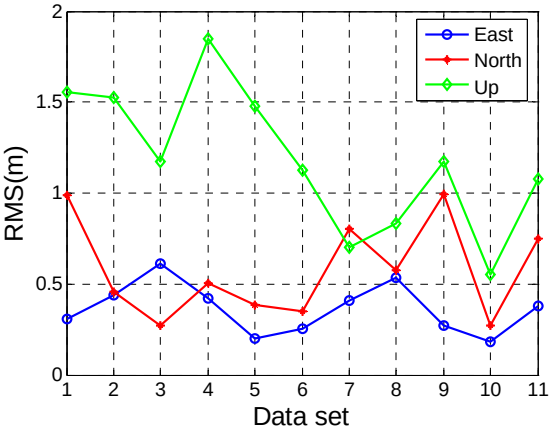

Figure 9: RMS of standalone GPS in 11 data sets for 1 hour operation

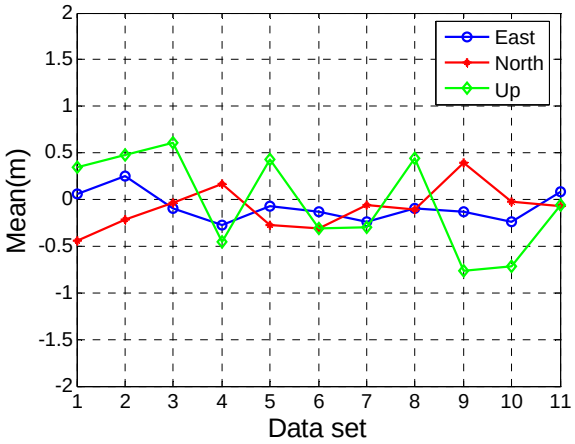

Figure 10: Mean of I-F PRP in 11data sets for 1 hour operation

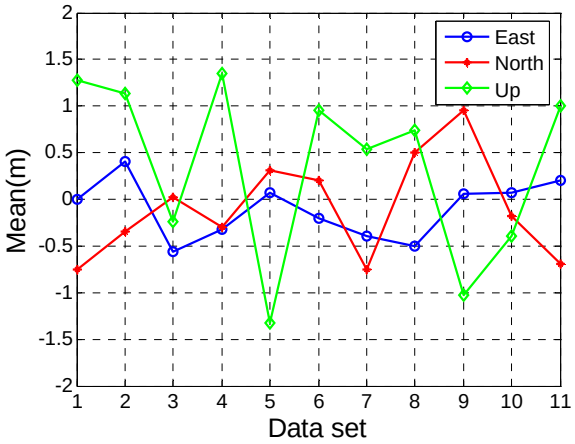

Figure 11: Mean of standalone GPS in 11 data sets for 1 hour operation

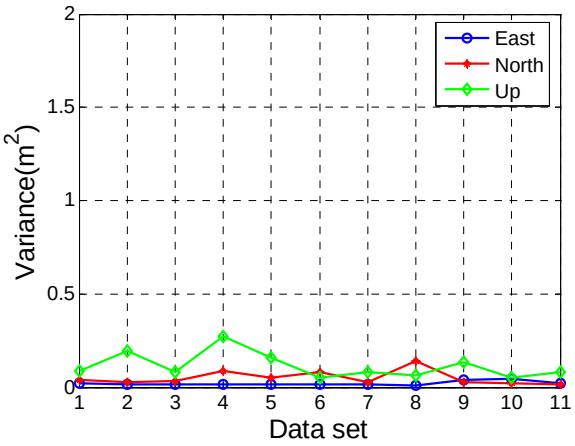

Figure 12: Variance of I-F PRP in 11 data sets for 1 hour operation

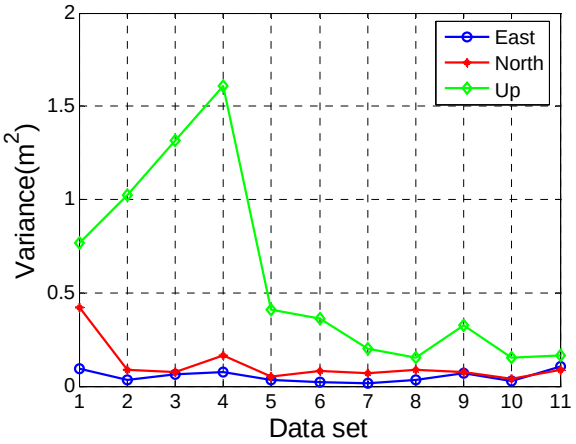

Figure 13: Variance of standalone GPS in 11 data sets for 1 hour operation

CONCLUSION

In this paper, a reference point-based precise relative positioning method is developed. It is assumed that a user can be equipped with only a single frequency receiver but can use other sensors in order to find the relative distance to a reference point at least one time during navigation. The absolute position of the reference point is assumed to be known to a user. In order to make the most of the known position of a receiver to the reference point, the two algorithms, I-F PRP and C-B PRP, are developed. The derivation of the two methods and the analysis of their expected error characteristics are discussed. Then, the two precise relative positioning methods are tested with the static data. The results of the tests show that the performance of C-B PRP, most of the time, is better than I-F PRP for 10 minutes of operation. Especially, C-B PRP supercedes I-F PRP near the beginning with less than 30cm position error in horizontal and less than 50cm in vertical for a few minutes of operation. I-F PRP provides better stability than standalone GPS for 1 hour of operation. The satellite constellation changes do not significantly degrade the performance of I-F PRP for the operation time. The rms of I-F PRP for 1 hour of operation is less than 50cm in horizontal and less than 1m in vertical.

These position errors do not take into account the offsets caused by other sensors when determining the relative position of a receiver to the reference point. Therefore, the overall accuracy of this method is the sum of the accuracy of the PRP and the accuracy of the other sensors. Since these results are obtained from the tests using the static data, a dynamic user may have slightly different results. This is especially true that if the short baseline assumption between a receiver and a reference point does not hold. It is also expected that the airborne users may have better results since multipath is usually less in the air

than on the ground. Users in an urban canyon will have worse results due to the severe multipath. It is promising that the combination of I-F PRP and C-B PRP can replace the expensive navigation grade INS in the current flight inspection system with a single frequency receiver.

ACKNOWLEDGMENTS

The authors gratefully acknowledge the support of FAA flight inspection division (AVN)

REFERENCES

1. Y. Yang, R.T. Sharpe, R.R. Hatch, NavCom Technology, Inc., "A Fast Ambiguity Resolution Technique for RTK Embedded within a GPS Receiver " *Proc. 2002 ION GPS*, Portland, Oregon, Sept. 2002
2. Donghyun Kim and Richard B. Langley, 'Instantaneous real-time cycle-slip correction for quality control of GPS carrier-phase measurements", *Navigation*: *J. Inst. Navigation*, Vol. 49, No. 4, winter 2002-2003
3. Gao, Y. and X. Shen (2002). "A New Method Of Carrier Phase Based Precise Point Positioning," *Navigation: Journal of the Institute of Navigation*, Vol. 49, No. 2.
4. Collins, J.P., R.B. Langley & J. LaMance (1996), "Limiting factors in tropospheric propagation delay error modelling for GPS airborne navigation". *52nd U.S. Institute of Navigation Annual Meeting*, Cambridge, MA, 19-21 Jun., 519-528.
5. Pratap Misra and Per Enge, "GLOBAL POSITIOINING SYSTEM: Signals, Measurements, and Performance", Ganga- Jamuna Press, 2001.